Pulsed Laser Photoacoustic Calorimetry of Metastable Species

Lewis J. Rothberg,† John D. Simon, Mark Bernstein, and Kevin S. Peters*

Contribution from the Department of Chemistry, Harvard University, Cambridge, Massachusetts 02138. *Received November 22, 1982*

Abstract: The first direct measurement of the heat of reaction of a metastable photochemical intermediate is described. The photoacoustic calorimeter is discussed in detail. The necessary theory upon which photoacoustic calorimetry is based is developed in the general case. A detailed discussion for the limiting cases of "long-lived" and "short-lived" transients is included. The heat of reaction of triplet benzophenone and aniline to form the metastable radical pair is found to be 46 ± 5 kcal/mol. This is in excellent agreement with the calculated thermodynamic enthalpy of 45 kcal/mol.

Understanding photochemical reactions has long been limited by the difficulty in establishing the energetics of many important intermediates. In some cases, luminescence reveals energy differences between emitting species and their corresponding ground states or reaction products, but this information is unavaliable for nonemitting species.

We have used gated photoacoustic detection[1] following picosecond laser excitation to obtain heats of reaction for formation of a nonemitting metastable intermediate, the radical pair formed in the photoreduction of triplet benzophenone by aniline (Scheme I). Although the amine photoreduction of benzophenone is perhaps the most studied and best understood of all photochemical reactions,[2] the heats of formation of the solvated radical and ion pairs have never been determined.

Since photoacoustic detection monitors nonradiative decay, it is ideally suited to calorimetric studies. Photoacoustic spectroscopy has been used to determine quantum yields for luminescence[3] and for intersystem crossing.[4] The phase shift between periodic excitation and the resulting photoacoustic signal has been used to make dynamical measurements,[5] but the interpretation of these results is not always straightforward. Though the "missing" energy due to photoinitiated chemical bond formation is perfectly analogous to that lost due to luminescence, to our knowledge this work represents the first time photoacoustic detection has been applied to evaluate an enthalpy change in a photochemical reaction.

In the present work, we analyze the photoacoustic signal which arises from the pulsed heat deposition following photoexcitation. We show that, in principle, one can deduce the history of heat deposition in a sample by analysis of the photoacoustic signal. It is thus possible to obtain both calorimetric and dynamic information, as well as to perform quantum yield measurements. In this study, we focus on quantitative calorimetric information and assume that the dynamics of the species examined have been independently determined. Our experimental results confirm the essential predictions put forth in the theoretical treatment of calorimetry of photogenerated metastable species. Finally, we illustrate the method with a measurement of the heat of reaction of the benzhydrol–amine radical pair formed in the photoreduction of benzophenone by aniline.

Theory

It is essential to understand how the pressure transducer signal reflects the original heat deposition profile in space and time. We consider a heat source function $h(\vec{r}',t')$ where $\vec{r}'$ and t' refer to the spacial and temporal source coordinates. Local thermal expansion initiates acoustic waves which obey the wave equation

$$\nabla^2\Psi(\vec{r},t) - \frac{1}{v_s^2}\frac{\partial^2\Psi(\vec{r},t)}{\partial t^2} = -4\pi h(\vec{r}',t') \qquad (1)$$

Scheme I

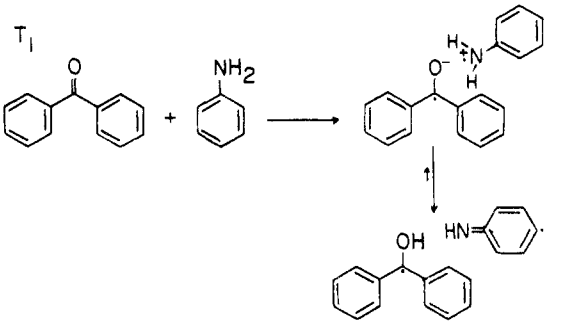

where v_s is the speed of sound in the (assumed to be dispersionless and linear) medium of interest and $\Psi(\vec{r},t)$ is the wave amplitude at the observer's coordinates $\vec{r},t$. The Green's function $g(\vec{r},\vec{r}',t,t')$ solves the wave equation for the impulse source $h(\vec{r}',t') = \delta(\vec{r} - \vec{r}')\delta(t - t')$. For our boundary conditions the solution is given by the causal retarded Green's function

$$g(\vec{r},\vec{r}',t,t') = \frac{\delta\left(t - t' - \frac{|\vec{r} - \vec{r}'|}{v_s}\right)}{|\vec{r} - \vec{r}'|} \qquad (2)$$

where δ denotes the Dirac Delta function. The solution of eq 1 for an arbitrary source $h(\vec{r}',t')$ is

$$\Psi(\vec{r},t) = \frac{1}{4\pi}\int dt' \int d\vec{r}' g(\vec{r},\vec{r}',t,t')h(\vec{r},t') \qquad (3)$$

For the case of a point source at $\vec{r}' = 0$,[6] the impulse source is given by $h(\vec{r}',t') = \delta(\vec{r}')f(t')$ where $f(t')$ describes the temporal behavior of the source. For a "point observer" at $\vec{r}_0$ ($|\vec{r}_0| \equiv r_0$), eq 3 gives the result

$$\Psi(\vec{r}_0,t) = \frac{f[t - (r_0/v_s)]}{4\pi r_0} \qquad (4)$$

Thus, in the case of a point source, the original heat source is converted to a pressure source at the detector. The pressure source has the same temporal profile as the original heat source but is characterized by both a propagation delay of r_0/v_s and the energy

†Current address: Harvard University, Division of Applied Physics, Cambridge, Mass. 02138.

*Camille and Henry Dreyfus Teacher–Scholar. Author to whom inquiries should be addressed.

(1) Patel, C. K. N.; Tam, A. C. *Rev. Mod. Phys.* **1981**, *53*, 517.
(2) (a) Simon, J. D.; Peters, K. S. *J. Am. Chem. Soc.* **1981**, *103*, 6403. (b) Cohen, S. G.; Parola, A. H.; Parsons, G. H., Jr. *Chem. Rev.* **1973**, *73*, 141. (c) Wagner, P. J., *Top. Curr. Chem.* **1976**, *66*, 1.
(3) (a) Adams, M. J.; Highfield, J. G.; Kirkbright, G F. *Anal. Chem.* **1977**, *49*, 1850. (b) Lahmann, W.; Ludewig, H. J. *Chem. Phys. Lett* **1977**, *45*, 177. (c) Rockley, M. G.; Waugh, K. M. *Ibid.* **1978**, *54*, 597. (d) Starobogatov, I. O. *Opt. Spectrosc. (Engl. Transl.)* **1977**, *42*, 172.
(4) Callis, J. B.; Gouterman, M.; Danielson, J. D. S. *Rev. Sci. Instrum.* **1969**, *40*, 1599.
(5) Harshbarger, W. R.; Robin, M. B. *Acc. Chem. Res.* **1973**, *6*, 329, and references cited therein.
(6) The criteria which delineate this case for the purpose of our experiments are discussed later.

0002-7863/83/1505-3464$01.50/0

conserving $1/r_0$ decay in amplitude always associated with spherical wave emitters. Of present interest to us is the nonradiative decay of a single transient of lifetime τ so that

$$f_\tau(t') = \frac{h_0 e^{-t'/\tau}}{\tau}\,\Theta(t') \tag{5}$$

where $\Theta(t')$ is a unit step (Heaviside) function beginning at $t' = 0$. The normalization factor $1/\tau$ is added so that the total heat deposition is given by

$$h_0 = \int\int h(\vec{r}',t')\,d\vec{r}'dt' \tag{6}$$

independent of τ. The wave amplitude at the detector is then

$$\Psi(\vec{r}_0,t'') = \frac{h_0}{4\pi r_0}\,\frac{e^{-t''/\tau}}{\tau}\Theta(t'') \tag{7}$$

where, for convenience, we have let the observer's time begin at retarded time $t'' = t' - (r_0/v_s)$. A transducer sensitive to longitudinal displacement waves (e.g., a piezoelectric microphone) converts $\Psi(\vec{r}_0,t'')$ to an electrical signal. We model such a detector as an underdamped oscillator whose impulse response (i.e., Green's function $G(t,t'')$)

$$G(t,t'') = A \sin(\nu(t - t''))e^{-(t-t'')/\tau_0} \tag{8}$$

has characteristic oscillation frequency ν and relaxation time $\tau_0 \gg 1/\nu$. Our piezoelectric transducer can be described qualitatively with $\nu \approx 1 \times 10^5$ Hz and $\tau_0 \approx 1$ ms, but the ensuing discusion does not depend critically on the number and details of the poles characterizing the transducer, and thus can be generalized to any linear network.

The detector response $V(t)$ for an arbitrary forcing function $\Psi(\vec{r}_0,t'')$ is given by convolving the impulse response with the forcing function:

$$V(t) = \int_{-\infty}^{t} G(t,t'')\Psi(\vec{r}_0,t'')\,dt'' \tag{9}$$

The signal due to the transient point source, $f_\tau(t')$, of heat-induced pressure waves can be expressed as:

$$V(t) = \frac{-h_0 A}{4\pi r_0 \tau}e^{-t/\tau}\int_0^t e^{-u/\tau'}\sin(\nu u)\,du \tag{10}$$

where we have let $u = t'' - t$ and $1/\tau' = (1/\tau) - (1/\tau_0)$. The result is that

$$V(t) = \frac{h_0 A}{4\pi r_0 \tau}\,\frac{\nu}{\nu^2 + (1/\tau)^2}\left\{e^{-t/\tau} - e^{-t/\tau_0}\left[\cos(\nu t) - \frac{1}{\nu\tau'}\sin(\nu t)\right]\right\} \tag{11}$$

For the particular case of interest where $\tau \ll \tau_0$, $1/\tau' \approx 1/\tau$, the above equation becomes:

$$V(t) = \frac{h_0 A}{4\pi r_0}\,\frac{\nu\tau}{1 + \nu^2\tau^2}\left\{e^{-t/\tau} - e^{-t/\tau_0}\left[\cos(\nu t) - \frac{1}{\nu\tau}\sin(\nu t)\right]\right\} \tag{12}$$

The maximum signal excursions for the limiting cases of "short-lived" transients ($\nu\tau \ll 1$) and "long-lived" transients ($\nu\tau \gg 1$) are given by

$$|V_{max}(\tau \ll 1/\nu)| \rightarrow \frac{h_0 A}{4\pi r_0}\,e^{-t/\tau_0} \tag{13}$$

$$|V_{max}(\tau \gg 1/\nu)| \rightarrow \frac{h_0 A}{4\pi r_0}\,\frac{1}{\nu\tau}(e^{-t/\tau} + e^{-t/\tau_0}) < \frac{h_0 A}{4\pi r_0}\,\frac{2e^{-t/\tau_0}}{\nu\tau} \tag{14}$$

Equations 13 and 14 embody the principle upon which photoacoustic calorimetry works. The signal due to short-lived transients is independent of τ, which is reasonable because the transducer cannot discriminate between pressure waves which are much faster than its response time, $1/\nu$. The maximum signal due to long-lived transients is smaller than that due to short-lived transients by a factor of order $1/\nu\tau$, where $\nu\tau \gg 1$. Dramatically less signal amplitude is induced by the same net heat deposition on timescales long compared to $1/\nu$ because the detector's sinusoidal "impulse" responses associated with different time slices of the arriving pressure waves can get out of phase in time $1/2\nu$ and destructively interfere. If the amplitude of the pressure wave has not decreased during this time (i.e., $e^{-1/2\nu\tau} \approx 1$ or $\nu\tau \gg 1$), then the signal is greatly diminished by almost complete interference.

The virtual absence of photoacoustic contributions from long-term transients enables one to consider calorimetric experiments which measure heat "lost" in forming metastable photochemical or photophysical transients (or products) with lifetimes $\tau \gg 1/\nu$. To perform these experiments, we assume that the samples of interest are dilute so that the acoustic properties depend exclusively on the environment (e.g., the solvent for solutions). We create short-lived transients of known nonradiative yield, Φ_{nr}, with photons of known energy, $E_0 = h\nu_{exc}$, in a sample of known absorbance, A. We then measure the signal amplitude corresponding to the known heat deposition, $h_0 = \Phi_{nr}E_0A$. This gives us the proportionality constant, $A/4\pi r_0$, between signal amplitude and heat deposition, resulting in an absolute calibration of our apparatus. Provided that the sample and transducer properties are linear, one can obtain the amount of heat *not* deposited at times $\tau \ll 1/\nu$ by an arbitrary sample of measured absorbance in the same environment as the calibration was done.

If the photophysical and photochemical dynamics following excitation are known, then the "missing" energy can be ascribed to luminescence and/or to formation of products or intermediates which do not decay on the experimental timescale. It is possible, for example, to measure heats of complex formation, heats of reaction, and heats of solvation of metastable species. In principle, one can (in the point source limit) obtain the exact temporal dependence of heat deposition, $f(t')$, by measuring the impulse response $G(t,t'')$ and then deducing $f(t')$ via eq 4 and 9 from the sample response $V(t)$. This process is easier to understand in the frequency domain, where we consider the Fourier transformed functions $\hat{\Psi}(\omega)$, $\hat{G}(\omega)$, and $\hat{V}(\omega)$. If we empirically determine both $\hat{V}(\omega)$ for a sample of interest as well as $\hat{G}(\omega)$, the apparatus response to a signal from a rapidly decaying species, then, from eq 9 and the convolution theorem,

$$\hat{\Psi}(\omega) = \hat{V}(\omega)/\hat{G}(\omega) \tag{15}$$

In practice, however, the narrow bandwidth of piezoelectric microphones severely restricts the applicability of this approach.

While it is pedagogically convenient to discuss the case of a point source and point detector, for realistic experiments it is not always convenient to meet these criteria. In fact, the experiments to be reported here do not meet these criteria. We therefore consider a more general case qualitatively, and show that the basic ideas delineated above hold for an extended source of acoustic waves under certain simple conditions. We retain the assumption of a point detector.

The correct pressure arrival function $\Psi(\vec{r}_0,t)$ is still obtained by the integration of eq 3, but now the solution is not expressible in closed form even in simple realistic geometries. The appropriate arrival function no longer mirrors the heat deposition in time because the extension of the sample causes different apparent arrival times for pressure waves which are generated simultaneously. When the spatial extent of the sample is such that waves emanating from different parts of the sample can arrive at the detector separated by more than $1/\nu$, then the point source approximation breaks down. If the source has characteristic dimension L, then the criterion for a point source is that the sample traversal time, L/v_s, be less than $1/\nu$. In the case of extended sources, even a very short-lived transient, $\tau \ll 1/\nu$, has an apparent lifetime $\tau_{eff} \approx L/v_s > 1/\nu$. Then short-lived transients no longer retain their advantage over long-lived ones because the effective lifetime τ_{eff} is long compared to the transducer response time ($\tau_{eff} > 1/\nu$). In our experiments, for example, $v_s \approx 10^5$ cm/s, $1/\nu \approx 10$ μs, and the source extension is roughly the beam path length in a cell of $L \approx 1$ cm. The sample traversal time is about 10 μs so that we are well into the extended source regime. However, as in the point source case we are still able to differentiate between

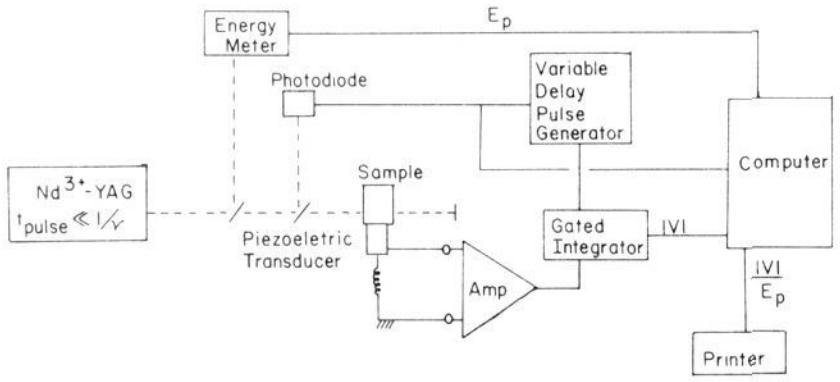

Figure 1. Schematic of the photoacoustic calorimeter used in this study.

short- and long-lived transients by measuring the photoacoustic amplitude at times t, $t < 1/\nu$. In this way we measure only waves arriving from the closest length, $L_{eff} = v_s t$ of the sample. This means that $L_{eff}/v_s < 1/\nu$, and the criterion presented above for a point source is satisfied. Therefore, the qualitative results in eq 13 and 14 continue to hold. Naturally, the extension of the source makes extrapolation to the intermediate case $\tau \approx 1/\nu$ impossible, but the range of τ not appropriately described by the limiting cases of eq 12 is small.

Experimental Section

A schematic of our apparatus appears in Figure 1. Optically thin sample solutions were excited by 25-ps pulses of 355-nm radiation produced by a Quantel YG-400 mode-locked Nd^{3+}–YAG laser. The beam enegy (≤0.1 mJ) and spot size (≈1.5 mm) were controlled to prevent nonlinear effects. A microcomputer continuously monitored the proportionality between laser power and observed signal; nonlinearity arising from stimulated Raman scattering was readily detected under more drastic conditions, but was completely absent in these experiments.

The photoacoustic transducer was based on the piezoelectric microphone devised by Tam and Patel.[1] The piezoelectric element was a lead zirconate–lead titanate cylinder, 4 mm in diameter and 4 mm in length (Transducer Products Corp. material LTZ-2), axially poled with silver electrodes, and was mounted within a polished stainless steel shell. The resonant frequency of the assembly was found to be approximately 100 kHz. The transducer was clamped against the side of a 1-cm quartz sample cuvette, and a thin layer of vacuum grease was applied between the transducer and the cuvette wall to minimize acoustic reflections at the interface.

The delay between excitation and the arrival of the leading edge of the photoacoustic pressure wave at the microphone clearly depends on the distance between the laser beam and the transducer. By varying this difference over a small range with a micrometer mount and measuring the change in arrival time of the photoacoustic wave, we determined the speed of sound in ethanol containing dilute rhodamine 6G to be 1300 ± 150 m/s, in agreement with the literature value of 1207 m/s.[7] This experiment verifies our assumption that the observed photoacoustic signals arise in the bulk sample and propagate through the solvent, excluding the possibility that signals are generated at the cuvette surface and propagate through the cuvette wall. All experiments were conducted at room temperature and atmospheric pressure. On the basis of the estimated microphone sensitivity of 3×10^{-5} V/(N/m^2),[1] the photoacoustically induced excess pressure wave does not exceed 10^{-2} atm anywhere in the sample, and thus represents a slight perturbation.

In each experiment, we observed stable and reproducible waveforms (Figure 2), with $1/\nu \approx 10$ μs and $\tau_0 \approx 1$ ms. As mentioned above, the effective sensitivity of the apparatus is a complex function of experimental geometry, which must therefore be held constant. The cuvette and transducer assembly were rigidly clamped, and the cell was cleaned and filled with care. The process of pipetting samples in and out of the sample cuvette did not alter the photoacoustic waveforms. Different dilute sample materials in the same solvent were also observed to produce identical waveforms, confirming our assumption that the acoustic properties of different samples were independent of solute. The observed amplitudes for all of the materials reported here were linear in solute concentration (absorbance) and in laser pulse energy.

The photoacoustic signal was amplified by a low-noise, high-impedance preamplifier derived from the design of Voigtman et al.,[8] with a gain of approximately 75 and a bandpass of approximately 10–500 kHz. Further amplification was provided by a homemade instrumentation amplifier (gain 2–250, 3 dB point above 400 kHz). The waveform was sampled for 1 μs during its first negative excursion by a gated integrator (Evans Associate Model 4130, modified to obtain a 1-μs time constant), and then read and recorded by the microcomputer controller[9] through an Analog Devices 0816 8-bit ADC.

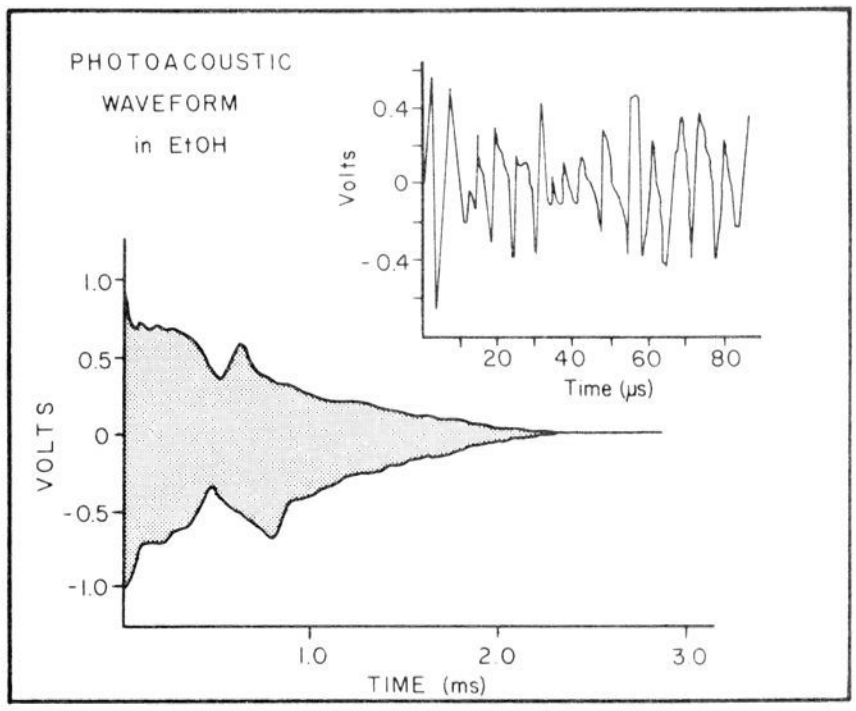

Figure 2. Experimental waveform for dilute rhodamine 6G in ethanol.

Table I. Quantum Yields and Normalized Calorimetric Information for the Standardization Compounds[a]

compound	Φ_f	$\bar{\nu}_f$ (cm^{-1})	Φ_{nr}	normalized $\lvert V\rvert/E_p A$
fluorenone	0.10	19 231	0.93	1.00
tetraphenylethylene	0.25	20 700	0.82	0.91
anthracene	0.36	24 900	0.68	0.84
rhodamine 6G	0.95	17 550	0.41	0.52
bis(*o*-methylstyryl)benzene	0.94	23 702	0.21	0.14

[a] Data are from ref 10.

After each laser shot, the microcomputer displayed the observed amplitude and the laser pulse energy, as measured by a Laser-Precision Rj-7200 energy meter using a RjP-735 pyroelectric probe. The normalized acoustic signal was calculated by dividing the photoacoustic voltage by the laser energy. The signal-to-noise ratio was sufficient to estimate the nonradiative quantum yield Φ_{nr} ($t \ll 1/\nu$) with a single pulse. To further reduce noise, the experiment was repeated at 10 Hz and results of 80 laser shots were averaged. The microcomputer was programmed to reject anomalously large and small laser pulses, and intermediate results were monitored to detect any indications of photodecomposition.

Aniline (Baker) was refluxed over KOH and distilled at reduced pressure under argon. Benzophenone (MCB) and anthracene (Aldrich) were purified by recrystallization. Fluorenone (Aldrich), rhodamine 6G (Exciton), tetraphenylethylene (Aldrich), and *p*-bis(*o*-methylstyryl)-benzene (Exciton) were used without further purification. Absolute ethanol (U.S. Industrial Chemical Corp.) was also used without further purification. For each compound to be studied, four solutions were mixed with absorbance at 355 nm ranging from 0.020 to 0.120. Sample absorbance was measured with a Perkin-Elmer Lambda 3 UV–vis spectrophotometer. For the solutions of benzophenone and aniline in EtOH, the concentration of benzophenone was varied but the aniline concentration for all solutions was 0.3 M. We found that a 0.3 M solution of aniline in ethanol gave no appreciable absorption at 355 nm, nor was any change in the waveform observed.

Results and Discussion

1. Calibration. In order to determine an absolute scale for calorimetric purposes, it is initially necessary to establish a quantitative correspondence between nonradiative energy deposition and photoacoustic amplitude. This was accomplished by examining ethanol solutions of the compounds listed in Table I. In air-saturated solutions, these compounds undergo little or no photochemical degradation, and give rise to no long-lived ($\tau \geq$

(7) "Handbook of Chemistry and Physics"; Weast, R. C., Ed.; CRC Press: Cleveland, 1975.

(8) Voigtman, E.; Jurgensen, A.; Winefordner, J. *Anal. Chem.* **1981**, *53*, 1442.

(9) Bernstein, M. *Byte* **1982**, *4*, 465.

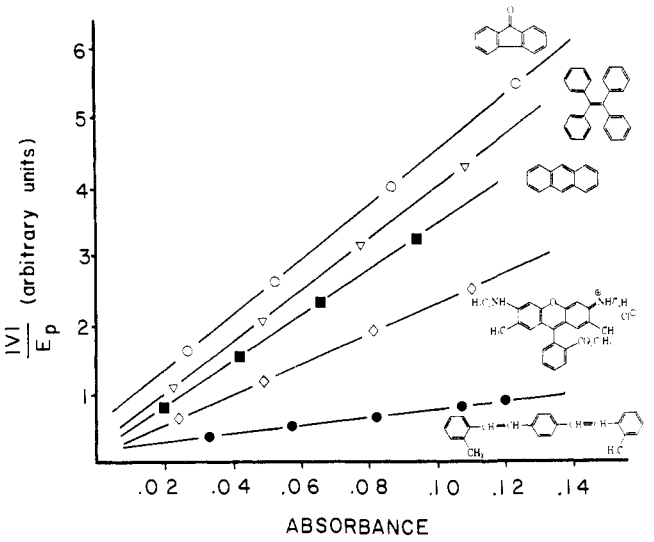

Figure 3. Normalized photoacoustic signal $|V|/E_p$ vs. solution absorbance for the calibration compounds (Table I): fluorenone (○), tetraphenylethylene (▽), anthracene (■), rhodamine 6G (◇), and *p*-bis(*o*-methylstyryl)benzene (●).

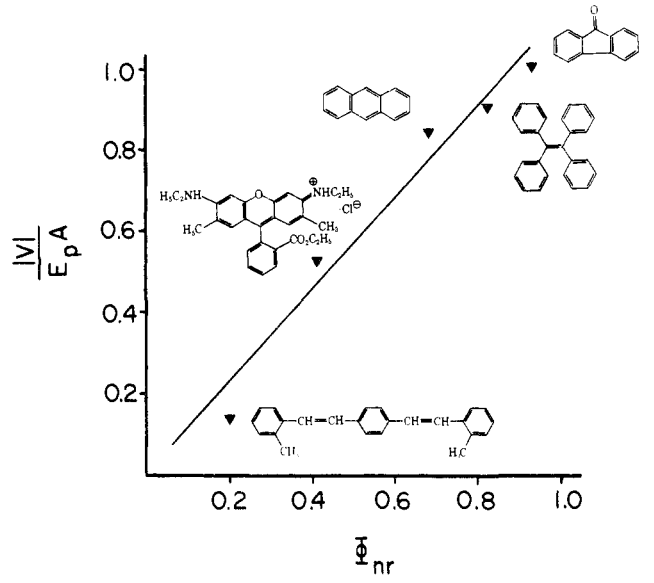

Figure 4. Instrumental calibration curve. Each point represents calorimetric data for one compound (Table I). In order of increasing Φ_{nr}, the compounds plotted are *p*-bis(*o*-methylstyryl)benzene, rhodamine 6G, anthracene, tetraphenylethylene, and fluorenone.

$1/\nu$) photophysical or photochemical intermediates. Excitation results in prompt release of heat accounting for all energy which is not radiated. Since their fluorescence quantum yields, Φ_f, and average fluorescence frequencies $\bar{\nu}_f$, are relatively well known,[10] we can calculate the fraction of absorbed energy deposited as heat, Φ_{nr}, using the following equation:

$$\Phi_{nr} = 1 - \Phi_f[\bar{\nu}_f/\nu_{exc}] \quad (16)$$

where ν_{exc} is the frequency of the excitation photon. The sample absorbs energy, E_pA (E_p is the laser pulse energy and A is the absorbance; $A \leq 0.12$ in the experiments reported in this paper), and the photoacoustic amplitude $|V|$ is proportional to the fraction, Φ_{nr}, of the energy converted to heat. That is,

$$|V| = K\Phi_{nr}E_pA \quad (17)$$

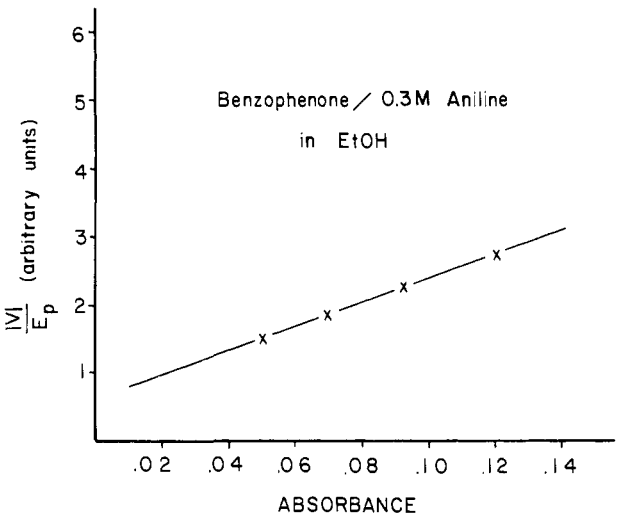

Figure 5. Normalized photoacoustic signal vs. solution absorbance for ethanol solutions of benzophenone/0.3 M aniline.

Scheme II

$(C_6H_5)_2C{=}O + H_2 \rightarrow (C_6H_5)_2CHOH$	$\Delta H = -9$ kcal/mol
$2H\cdot \rightarrow H_2$	$\Delta H = -104$ kcal/mol
$(C_6H_5)_2CHOH \rightarrow H\cdot + (C_6H_5)_2\dot{C}{-}OH$	$\Delta H = 78$ kcal/mol
$\text{aniline} \rightarrow C_6H_5\dot{N}H + H\cdot$	$\Delta H = 80$ kcal/mol
$(C_6H_5)_2C{=}O + \text{aniline} \rightarrow C_6H_5\dot{N}H + (C_6H_5)_2\dot{C}OH$	$\Delta H = 45$ kcal/mol

where K characterizes the apparatus geometry and gain. Figure 3 shows the normalized photoacoustic amplitude, $|V|/E_p$, plotted against absorbance for the calibration compounds. The linearity confirms the validity of the reasoning behind eq 17. The small deviation from zero intercept is due to slight window absorption and deliberate amplifier offset to permit the use of a unipolar analog-to-digital converter. In Figure 4, the slopes of the lines in Figure 3, $K\Phi_{nr}$, $K\Phi_{nr} = |V|/E_pA$, are graphed as a function of the calculated Φ_{nr} from Table I. The linearity of this plot is well within experimental error, and deviations are most probably due to uncertainties in the measured fluorescence yields. The calibration line of Figure 4 allows us to relate the measured slope, $|V|/E_pA$, of an arbitrary sample in ethanol to a nonradiative quantum yield Φ_{nr} ($t \ll 1/\nu$) for rapid nonradiative energy deposition.

2. Benzhydrol–Amine Radical Pair. The calibration curve of Figure 4 can now be applied to the reaction of Scheme I, the photoreduction of benzophenone by aniline in air-saturated ethanol. Following 355-nm photoexcitation, benzophenone changes to triplet benzophenone with unit quantum yield within 10 ps.[11] From time-resolved absorption studies,[12] it is known that triplet benzophenone reacts quantitatively with aniline within 5 ns to form the benzhydrol–amine radical pair. Independently measured values of the relative extinction coefficients of triplet benzophenone and the radical pair also indicate that triplet benzophenone reacts with aniline to form the radical pair in unit quantum yield.[12] These results indicate that the formation of singlet oxygen resulting from oxygen quenching of benzophenone is negligible under our experimental conditions.

Once the radical pair is formed, it undergoes essentially no decay on the experimental timescale[12] before reverting to its original constituents[13] Therefore the heat of reaction associated with the decay of the radical pair does not contribute to the photoacoustic signal. Since nearly all (>99%) of the benzophenone triplet phosphoresence is quenched by the rapid reaction with aniline,

(10) (a) Wilkinson, F. "Organic Molecular Photochemistry"; Birks, J. B., Ed.; Wiley: New York, 1975; Vol. 2, p 95. (b) Berlman, I. B. "Handbook of Fluorescence Spectra of Aromatic Molecules", 2nd ed.; Academic Press: New York, 1971. (c) Sharafy, S.; Muszkat, K. A. *J. Am. Chem. Soc.* **1971**, *93*, 4119. (d) Yoshihara, K.; Kearns, D. R. *J. Chem. Phys.* **1966**, *45*, 1991.

(11) Greene, B. I.; Hochstrasser, R. M.; Weisman, R. B. *J. Chem. Phys.* **1979**, *70*, 1247.

(12) Simon, J. D.; Peters, K. S. *J. Am. Chem. Soc.*, submitted for publication.

(13) (a) Inbar, S.; Linschitz, H.; Cohen, S. G. *J. Am. Chem. Soc.* **1980**, *103*, 1048. (b) Simon, J. D.; Peters, K. S. *Ibid.*, submitted for publication.

the mising energy can all be attributed to formation energy of the radical pair.

Measuring a series of benzophenone/0.3 M aniline samples in EtOH, we observe the slope, $|V|/E_pA$ in Figure 5 corresponding to $\Phi_{nr} = 0.43 \pm 0.06$. The heat of reaction is then just $(1 - \Phi_{nr})h\nu_{exc} = 46 \pm 5$ kcal/mol. The error in the absolute value of the reaction heat results mostly from uncertainty in the calibration curve of Figure 5. Although the error in the absolute value is quite substantial, the internal consistency of our data allows us to assign relative nonradiative yields to better than 0.01.

The measured value of heat of reaction to the radical pair, 46 ± 5 kcal/mol, is in good agreement with the enthalpy of reaction deduced from the thermodynamic cycle of Scheme II.[14] Since the system being studied is not at equilibrium the value that we obtain experimentally is not rigorously the thermodynamic enthalpy of reaction. However, the photoacoustic wave does not significantly alter the pressure of the system; the experiment is performed at nearly constant pressure. Thus, we would expect to obtain good agreement between our measured value and the calculated enthalpy change.

Conclusions

In this paper we report the first direct measurement of the heat of reaction of a metastable photochemical intermediate, the radical pair produced by the reaction of triplet benzophenone with aniline. The pulsed photoacoustic technique used to measure nonradiative energy deposition is both simple and inexpensive. We have demonstrated both theoretically and experimentally that one can obtain quantitative calorimetric information directly by discriminating between heat deposited by long-lived ($\nu\tau \gg 1$) and short-lived ($\nu\tau \ll 1$) transients. In principle, both dynamic and calorimetric information can be obtained in the true point source limit. We have shown, however, that it is not necessary to design experiments to conform to this limit in order to retain calorimetric information.

In addition to the study of solution-phase calorimetry of other metastable species, extension of this work to the study of energy-transfer processes and gas-phase reactions is in progress. We have already used a two-color version of this experiment to measure the intensity-dependent quantum yields and the cross sections for stimulated emission of coumarin dyes.[15]

Acknowledgment. This work is supported by a grant from the National Science Foundation CHE-8117519, and the Camille and Henry Dreyfus Foundation.

Registry No. Aniline, 62-53-3; benzophenone, 119-61-9; fluorenone, 486-25-9; tetraphenylethylene, 632-51-9; anthracene, 120-12-7; rhodamine 6G, 989-38-8; *p*-bis(*o*-methylstyryl)benzene, 13280-61-0.

(14) (a) Walling, C.; Gibian, M. *J. Am. Chem. Soc.* **1965**, *87*, 3361. (b) See ref 7.

(15) (a) Rothberg, L. J.; Bernstein, M.; Peters, K. S. "Picosecond Phenomena III"; Eisenthal, K. B., et al., Eds.; Springer Verlag: New York, 1982, Vol. 23. (b) Rothberg, L. J.; Bernstein, M.; Peters, K. S. *J. Chem. Phys.*, accepted for publication.

Adsorption and Hydrogenation of Acetylene on Cu(110) and Cu(110)–O Surfaces

Duane A. Outka, C. M. Friend,† Scott Jorgensen, and R. J. Madix*

Contribution from the Departments of Chemical Engineering and Chemistry, Stanford University, Stanford, California 94305. *Received September 20, 1982*

Abstract: The chemistry of acetylene adsorbed at a temperature of 170 K on Cu(110) surfaces has been studied as a function of C_2H_2 and oxygen coverage using TPD, TPRS, X-ray PES, UV PES, isotope exchange reactions, AES, and LEED. Acetylene was largely nondissociatively adsorbed on clean Cu(110) with acetylene desorption peaks at 280, 340 and 375 K. Some ethylene formation was detected with a desorption maximum occurring at 340 K. Approximately 11% of the carbon initially adsorbed in the acetylene remained on the surface following ethylene desorption as determined using X-ray PES. Coadsorption of surface hydrogen atoms and acetylene on the Cu(110) surface increased the amount of ethylene formed, and the C_2H_2 which normally desorbed at 340 and 375K was completely hydrogenated to ethylene in the presence of excess surface hydrogen. The C_2H_2 temperature-programmed desorption spectrum obtained following adsorption on the Cu(110)–O surfaces was qualitatively the same as on the clean Cu(110) surface. The extent of acetylene dehydrogenation was greater on the oxidized surface by a factor of 3, indicating that oxygen facilitated acetylene dissociation. Indeed X-ray PES results showed a strong interaction between adsorbed oxygen and acetylene, whereas no such interaction was observed in the X-ray PES of C_2H_4 and $O_{(ads)}$. Water was formed by reaction of $C_2H_{2(a)}$ with $O_{(a)}$ in the temperature range of 200–400 K, and no ethylene formation was detected on the Cu(110)–O surfaces, since the surface hydrogen was removed by adsorbed oxygen to form water.

Introduction

The determination of the adsorption properties of hydrocarbons on clean and chemically modified transition metal surfaces may lead to a fundamental understanding of catalytically important surface processes. Basic ultra-high-vacuum studies may identify important surface intermediates in hydrocarbon reactions and the role of surface impurities in catalytic processes. Acetylene is one of the most widely studied cases of hydrocarbon adsorption and reaction on transition metal surfaces. Acetylene has been a molecule of choice because of its relative structural simplicity and the richness of its catalytic chemistry. To date, acetylene adsorption has been primarily studied on clean transition metal surfaces. Acetylene adsorption on nickel, palladium, and platinum surfaces has been studied with a wide range of ultra-high-vaccum techniques, including UV PES,[1-5] TDS,[1,4-6] EELS,[7-10] and

†Department of Chemistry, Harvard University, Cambridge, MA 02138.

(1) J. E. Demuth, *Surf. Sci.*, **93**, 127 (1980).
(2) K. Horn, A. M. Bradshaw, and K. Jacobi, *J. Vac. Sci. Technol.*, **15**, 575 (1978).
(3) T. E. Fischer and S. R. Keleman, *Surf. Sci.*, **74**, 47 (1978).
(4) J. E. Demuth, *Surf. Sci.*, **80**, 367 (1979).
(5) J. E. Demuth, *Surf. Sci.* **69**, 365 (1977).
(6) E. L. Muetterties, M.-C. Tsai, and S. R. Keleman, *Proc. Natl. Acad. Sci. U.S.A.*, **78**, 6571 (1981).

0002-7863/83/1505-3468$01.50/0